Pediatr Nephrol (1993) 7: 163–172

Pediatric Nephrology

Original article

Renal and biliary abnormalities in a new murine model of autosomal recessive polycystic kidney disease

Jeroen Nauta[1, 2], Yuko Ozawa[2], William E. Sweeney Jr[2], Joe C. Rutledge[3], and Ellis D. Avner[2]

[1] Department of Pediatrics, Sophia Children's Hospital, Rotterdam, The Netherlands
Departments of [2] Pediatrics and [3] Laboratory Medicine, Children's Hospital Medical Center and the University of Washington School of Medicine, Seattle, Washington, USA

Received June 11, 1992; received in revised form October 28, 1992; accepted November 3, 1992

Abstract. Current models of autosomal recessive polycystic kidney disease (ARPKD) fail to demonstrate biliary abnormalities in association with renal cysts. We therefore studied a new murine model of ARPKD in which dual renal tubular and biliary epithelial abnormalities are present. Affected homozygous animals typically die 1 month postnatally in renal failure with progressively enlarged kidneys. Renal cysts shift in site from inner cortical proximal tubules at birth to collecting tubules 20 days later, as determined by segment-specific lectin binding. Increased numbers of mitosis were demonstrated in proximal and collecting tubular cysts. In addition, epithelial hyperplasia was demonstrated morphometrically in the intra- and extrahepatic biliary tract of affected animals. The number of intrahepatic biliary epithelial cells was increased by 50% on postnatal day 5 and by 100% on postnatal day 25 ($P < 0.01$). Despite an increased frequency of "chaotic" portal areas in mice with renal cysts, no intrahepatic cysts or shape abnormalities of the biliary lumen were detected using biliary casts and morphometry. Additionally there was nonobstructive hyperplastic dilatation of the extrahepatic biliary tract which was linked in all animals to the presence of renal cysts. The hyperplastic abnormalities in both renal and biliary epithelium make this new mouse strain a good model for the study of the dual organ cellular pathophysiology of ARPKD.

Key words: Cystic kidney disease – Congenital hepatic fibrosis – Animal models – BPK mouse

Introduction

Autosomal recessive polycystic kidney disease (ARPKD) is a congenital disorder generally leading to end-stage renal failure within the perinatal period or early childhood. The disease is highly associated with hepatic abnormalities which can lead to cholangitis and portal hypertension [1–5]. The expression of disease in both kidney and liver is variable and has led to a number of different disease classifications [6–8]. On the basis of extensive family and clinical studies, it now appears that ARPKD is a single autosomal recessive disease complex with a wide clinical spectrum in which renal cystic disease is linked to biliary tract abnormalities and congenital hepatic fibrosis (CHF) [9, 10]. This disease complex includes the clinical entities previously classified as infantile polycystic disease, juvenile polycystic kidney disease, ARPKD, autosomal recessive polycystic liver disease, biliary duct ectasia, Caroli's disease and CHF. In the different clinical entities of this disease complex, liver lesions are variable. They consist of proliferation and dilatation of intrahepatic and sometimes extrahepatic bile ducts in conjunction with progressive fibrosis of portal connective tissue [9, 11]. Epithelial hyperplasia seems to be a hallmark for both hepatic and renal abnormalities [12, 13]. In both organs hyperplasia may be related to the expression of abnormal developmental programs [11, 14, 15].

Studies into the mechanisms of the formation and progressive enlargement of renal cysts have focused largely on animal models [16]. The C57BL/6J cpk/cpk (CPK) mouse has attracted considerable interest as a genetic model for ARPKD [12, 17, 18]. However the absence of hepatic lesions in affected animals is an important shortcoming of this model. Hepatic lesions have thus far only been identified in aged CPK animals which are heterozygous for the cystic trait [19, 20]. In the current study, we describe a new mutant strain of Balb/c mice in which ARPKD is expressed in conjunction with abnormalities of the intra- and extrahepatic biliary system.

Materials and methods

Animals. In 1985 polycystic kidney disease was recognized in an inbred strain of otherwise healthy Balb/c mice at the National Institutes of

Correspondence to: E. D. Avner, Children's Hospital and Medical Center, 4800 Sand Point Way, N.E., Seattle, Washington 98105, USA

Health. These animals were subsequently maintained as an inbred strain for over 25 generations at the University of Minnesota and expressed renal cystic disease as a stable autosomal recessive trait. In 1990 heterozygous breeding pairs from the Minnesota colony were obtained from Dr. R. Vernier and an inbred colony was established at the University of Washington. In the current study affected homozygous BPK (*B*alb/c *P*olycystic *K*idneys) mice were obtained from the controlled breeding of animals known to be heterozygous for the cystic disease. Wild type Balb/c mice (Simonsen Laboratories Gilroy, Calif., USA) served as controls. All animals were fed standard mouse chow containing 24% protein.

Light microscopy. For histological analysis, kidneys were obtained from cystic and control animals on postnatal days 0, 5, 10, 15, 20 and 25. Livers were obtained on postnatal days 5, 15 and 25. No livers were included on day 0 because identification of bile ducts proved to be inaccurate at this age due to the immaturity and small size of the ducts and the relatively heterogenous background caused by extensive hematopoetic activity. Histological analysis of the liver sections was performed blind by an experienced pediatric pathologist (J.R.). Other structures and organs were studied at only one postnatal age. Heart, sternum, spleen, brain, intestine and salivary gland were obtained on day 25, which is the age of terminal disease in BPK mice. Gallbladders, common bile ducts, choledochoduodenal junctions and pancreases were studied on day 10 when the moderately enlarged kidneys do not cause mechanical obstruction of the biliary tract.

The tissue was fixed in 3.5% paraformaldehyde for 30 min at 4° C, washed, dehydrated in graded acetone, infiltrated and embedded in Immunobed plastic embedding medium (Polysciences, Warrington, Pa., USA). Sections of 3 μm were mounted on glass and stained with hematoxylin. Staining for bilirubin was also performed, using Fouchet's reagent, on paraffin-embedded liver sections from 10-day-old mice.

Immunolocalization. Cyst localization was studied by segment-specific lectin binding using *Dolichos biflorus* agglutinin (DBA) as a marker for collecting tubules and *Lotus tetragonolobus* agglutinin (LTA) as a marker for proximal tubules [21, 22]. Renal cysts from 6 BPK mice per age group on days 0, 5, 10, 15 and 20 postnatally were lectin profiled at three different depths of the tissue following standardized embedding and serial sectioning. Depths were chosen as 10%, 30% and 50% of the thickness of each embedded kidney. In each section all cysts were classified as either DBA positive, LTA positive, or negative for both LTA and DBA. No cysts were positive for both lectins.

Biliary tract epithelium was identified utilizing a rabbit polyclonal antibody against human cytokeratin (Accurate Chemical and Scientific), which has reactivity with developing rodent biliary epithelium as previously demonstrated [23].

The immunostaining procedure used was our previously described postembedding technique specifically developed for immunolocalization of antigens and lectins in plastic sections of developing murine tissue [24, 25]. Etched and trypsinized Immunobed sections were incubated overnight at 4° C followed by 30 min at room temperature with either biotinylated lectins (6.25 μg/ml for LTA and DBA, Sigma) or, after blocking with normal goat serum (1 : 50 for 30 min), with the cytokeratin antibody (1 : 250). This was followed for lectins by avidin-peroxidase (1 : 500) for 90 min and for antibody staining by sequential incubations with bridging goat anti-rabbit IgG (1 : 40) for 90 min and rabbit peroxidase-antiperoxidase complex (1 : 100) for 45 min. Sections were then stained with 0.05% diaminobenzidine, 0.01% hydrogen peroxide and counterstained with hematoxylin.

Mitotic indices. Mitotic figures in both cystic and normal tubular walls were counted in lectin-stained kidney sections from 0-, 5-, 10- and 20-day-old BPK and control mice. The tissue was fixed, embedded in plastic and stained with segment-specific lectins as described in the section on immunolocalization. We analyzed 6 mice per age group. Data were obtained at three different depths at 10%, 30% and 50% of the thickness of the tissue and pooled for each kidney. Data are expressed as mitotic indices, being defined as the mean number of mitotic figures per 1,000 cells in each group.

Counting of portal structures and bile duct morphometry. Due to the patterned arborization of the biliary tract, it was essential to standardize depth and angle of liver sections for histological and morphometric analysis. In each case the major left lobe was embedded with the convexity to the surface of the plastic. Sections were cut parallel to the surface of the liver at a depth of 30% of the liver thickness. In this manner a standardized population of peripheral and more central bile ducts was consistently obtained. Sections from control and BPK livers were examined blind by the observer (J.N.) prior to analysis. Structures were counted in one liver section from each of 5–7 animals from both control and BPK groups on postnatal days 5, 15 and 25. In each section all veins, portal areas, bile ducts and biliary epithelial cells were counted. A portal area was identified when a vein was accompanied by at least one bile duct. A biliary epithelial cell was defined as an epithelial cell lining a bile duct. In addition computer-assisted morphometric analysis (Sigmascan) was performed on days 15 and 25 on the same coded sections as used for the counting of structures. Surface area of the section and surface area and circumference of each bile duct lumen were analyzed, as well as a size-independent measure of circularity of bile duct profiles. This "shape factor" was defined as the square root of the surface area divided by the circumference [26].

Electron microscopy. For electron microscopy, representative samples of kidney, liver and common bile duct obtained on postnatal days 5, 15 and 25 were fixed in a mixture of 2% paraformaldehyde/2.5% glutaraldehyde for 2 h at 4° C and postfixed in 0.5% osmium tetroxide for 1 h at 4° C. The tissue was then dehydrated through a series of graded acetone and infiltrated and embedded in Spurr (Polysciences). Ultrathin sections were mounted on copper mesh grids and stained with uranyl acetate and lead citrate.

Microfil casts of the biliary tract. Casts of the biliary tract of 3 control and 3 BPK animals of 20 days of age were made using yellow silicone rubber (Microfil, Canton Bio-Medical Products, Boulder, Colo., USA). This age was chosen in order to permit the study of potential liver lesions as late as possible during their development prior to the stage of terminal renal disease. The common bile duct was punctured with a 30-gauge needle and silicone rubber infused into the biliary tract under a pressure of 30 cm H_2O. The duct was ligated after the rubber was visualized in the distal duct radicals using a stereomicroscope. The liver was fixed in graded alcohol, digested in 1% potassium hydroxide, further cleared in a 1 : 1 mixture of glycerin and 70% ethyl alcohol and examined for cystic dilatations by stereomicroscopy.

Pressure-flow study on choledochoduodenal junctions. In addition to the study of cholestatic features by serum biochemistry, light microscopy and electron microscopy, pressure-flow studies of the choledochoduodenal junction were performed in a limited number of 10-day-old animals. At this age, bile duct cannulation was technically feasible. Unlike older mice, interference of the progressively enlarging kidneys with the bile flow could be excluded at this stage. In 4 control and 4 BPK mice, the outflow resistance of the common bile duct was calculated from a pressure-flow study using constant pressure [27]. The BPK mice presented with massive dilatation of the extrahepatic biliary tract typically present in all affected animals. The flow of 0.9% saline at a constant pressure of 30 cm H_2O through a 30-gauge needle was measured and the resistance calculated and reduced by the baseline resistance of the needle. This baseline resistance was 25 ± 2 cm $H_2O/\mu l$ per second and constant in the pressure range from 10 to 50 cm H_2O. During these experiments the duodenum was opened in order to permit free outflow. Backflow into the pancreatic duct was never observed.

Blood chemistry. Plasma urea nitrogen values were obtained from 9 control animals and from 11 BPK animals at three distinct postnatal developmental stages. Plasma conjugated and unconjugated bilirubin measurements were performed on day 10 in 6 control and 5 BPK animals. Samples were analyzed by Kodak Ektachem 700 spectrophotometry.

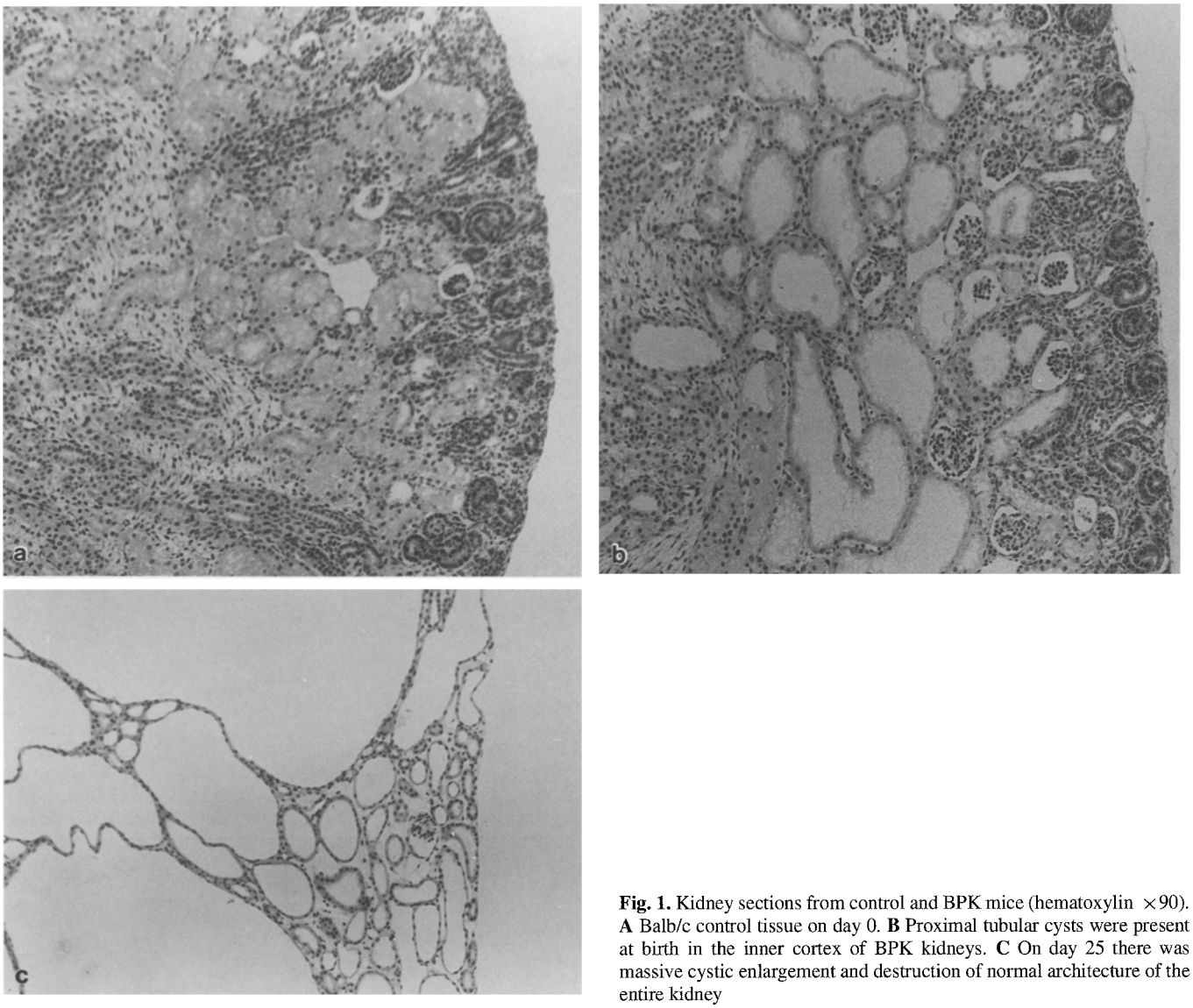

Fig. 1. Kidney sections from control and BPK mice (hematoxylin ×90). **A** Balb/c control tissue on day 0. **B** Proximal tubular cysts were present at birth in the inner cortex of BPK kidneys. **C** On day 25 there was massive cystic enlargement and destruction of normal architecture of the entire kidney

Statistics. Data are expressed as means and standard deviations. Differences between control and BPK animals studied at a single time point were analyzed by a paired two-tailed *t*-test. Strain effects studied at multiple time points were analyzed by analysis of variance. When significant overall strain effects were present, the Bonferroni method of adjustment for multiple comparisons was used to determine the specific ages at which this effect was significant. An effect was considered to be significant when $P < 0.05$.

Table 1. Localization of renal tubular cysts during cystogenesis as a percentage of total cysts[a, b]

Age (days)	Proximal	Collecting	Unclassified
0	97 (3)	0	3 (3)
5	73 (5)	13 (3)	14 (5)
10	58 (6)	23 (5)	19 (6)
15	38 (5)	46 (4)	16 (4)
20	11 (4)	78 (7)	11 (3)

[a] According to segment-specific lectin binding
[b] Expressed as mean with SD in parentheses

Results

Clinical

In a series of 219 mice born from proven breeding pairs, 21% were found to be affected by the cystic trait. This percentage was relatively stable (20%–25%) over a 5-year period of inbreeding at the University of Minnesota and the University of Washington. Males and females were equally affected. At birth affected BPK mice were clinically normal and subsequently developed progressive renal enlargement with massive abdominal distension, which was detectable in all affected mice by physical examination at the age of 2 weeks. Renal failure and death followed at the age of 4 weeks. At the ages of 2 and 4 weeks, plasma urea values of affected animals deviated significantly and progressively from control values (at day 15, 31 ± 9 vs. 18 ± 1 mg/dl, $P < 0.01$ and at day 25, 88 ± 14 vs. 24 ± 4 mg/dl, $P < 0.01$). Plasma bilirubin was not different in the 10-day-old BPK and control animals (0.08 ± 0.11 vs.

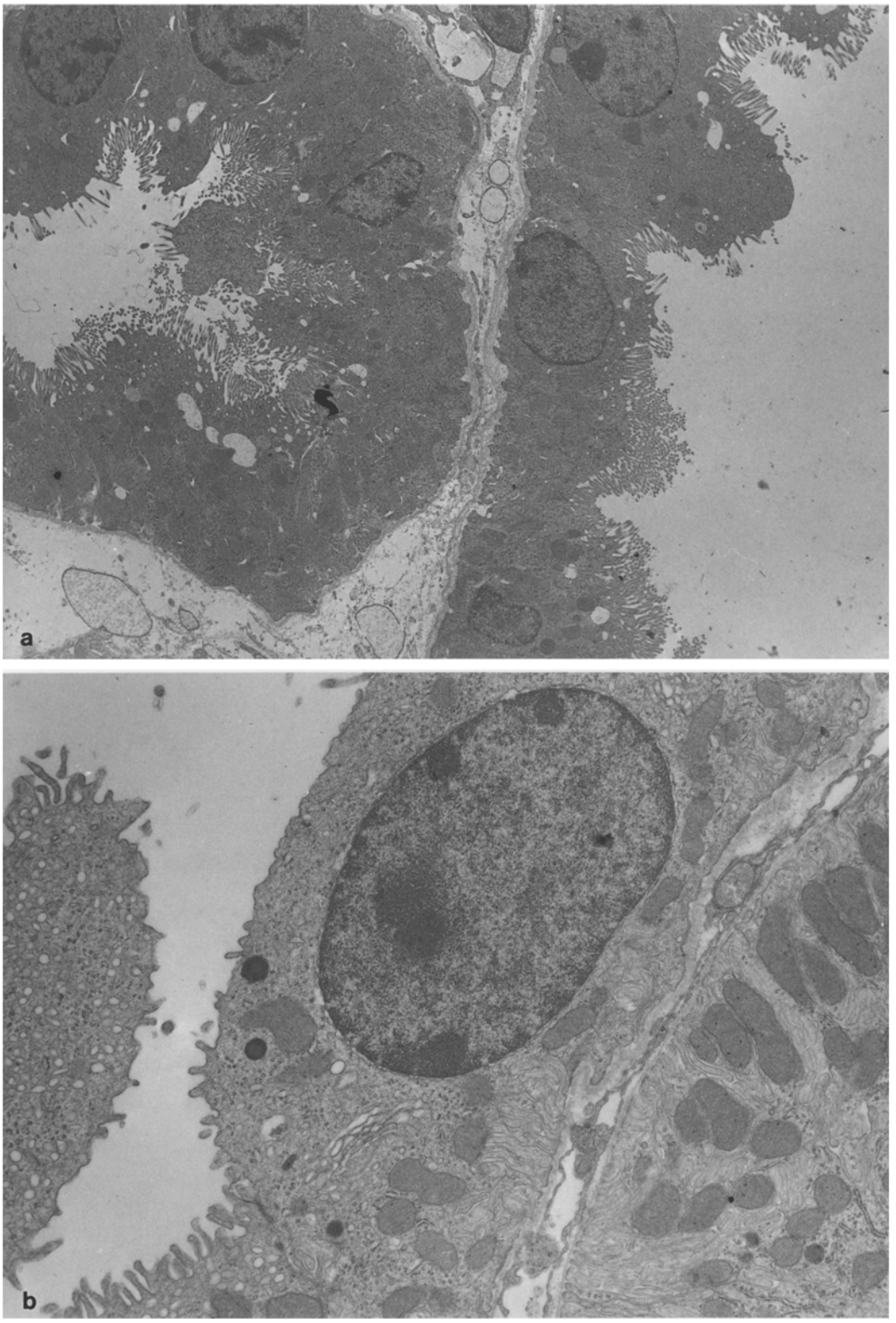

Fig. 2A, B

Fig. 2. Transmission electron microscopy of renal lesions on day 5 and 25. **A** Proximal tubules of a 5-day-old BPK mouse. One appears normal and the other is dilated forming a cyst. The lining cells of the dilated tubule maintain proximal tubule characteristics similar to those of the normal tubule which include microvilli, an apical-vacuolar network, normal intracellular organelles, basal nuclei and a regular basal lamina (×5,300). **B** Collecting tubule of Balb/c control on day 25 demonstrates a principal cell (*center*), including a fairly smooth apical membrane, extensive infoldings of the basal region, a lack of lateral cell processes and interdigitations, scarce mitochondria which are scattered randomly in the cytoplasm and, in contrast to the neighboring intercalated cell (*right*), a lack of apical tubulovesicular membrane structures (×13,300). **C** Collecting tubular cyst of BPK on day 25. Cyst-lining cells with morphological characteristics of principal cells. Organelle numbers and basal organization are decreased compared with controls (×5,300)

Table 2. Mitotic indices in renal tubules and cysts[a, b]

Age (days)	Proximal tubules			Collecting tubules		
	Control tubules	BPK noncystic tubules	BPK cystic tubules	Control tubules	BPK noncystic tubules	BPK cystic tubules
Day 0	3.9 (0.6)	3.7 (0.5)	9.3 (1.3)*	4.1 (0.5)	3.6 (0.8)	
Day 5	4.0 (1.1)	5.5 (2.7)	7.5 (1.5)*	2.5 (1.0)	4.0 (1.4)	7.2 (1.6)*
Day 10	4.8 (1.2)	5.3 (1.6)	5.3 (1.9)	2.5 (1.2)	3.2 (1.3)	7.3 (1.7)*
Day 20	3.2 (1.2)	3.7 (1.3)	4.3 (1.3)	2.2 (1.5)		3.8 (1.1)

* $P < 0.05$ compared with control tubules

[a] Mitotic indices = mitotic figures per 1,000 cells

[b] Mean with SD in parentheses of mitotic indices in lectin-defined proximal and collecting tubular segments of control and homozygous BPK mice

0.18 ± 0.13 mg/dl for conjugated bilirubin and 0.02 ± 0.02 vs. 0.03 ± 0.05 mg/dl for unconjugated bilirubin).

Kidneys

Morphological alterations in BPK kidneys were present at all postnatal stages (Fig. 1). At birth they consisted of tubular dilatations and early cyst formation in the inner cortical zone. During successive postnatal stages, tubules underwent progressive cystic enlargement, with consequent nephron destruction. During postnatal life there was a gradual shift in site of cystic nephron involvement, from proximal tubules to collecting tubules, as defined by lectin binding (Table 1). A small proportion of the cysts did not bind LTA or DBA. Binding of both LTA and DBA never occurred in the same cysts.

Ultrastructurally, cyst lining epithelial cells from 5-day-old affected animals were unremarkable and normally differentiated compared with age-matched controls (Fig. 2A). Most cysts were lined by cells with the morphology of normal proximal tubules. Microvilli were well formed and cell junctions, basal lamina and the distribution of cell organelles were normal. In 15-day-old animals the cyst lining cells were slightly flattened and had fewer and shorter microvilli in cysts of both proximal and collecting tubules. The apical cell junctions and the interdigitating pattern of cell-cell contacts were normal. Compared with controls, the mitochondria were decreased in number and slightly swollen as were the apical microvesicles. By day 25, cyst lining cells were even more flattened and microvesicles rare (Fig. 2B, C). Proximal tubular characteristics were rarely seen in direct correlation with the lectin profiling studies. Most cyst-lining epithelium had

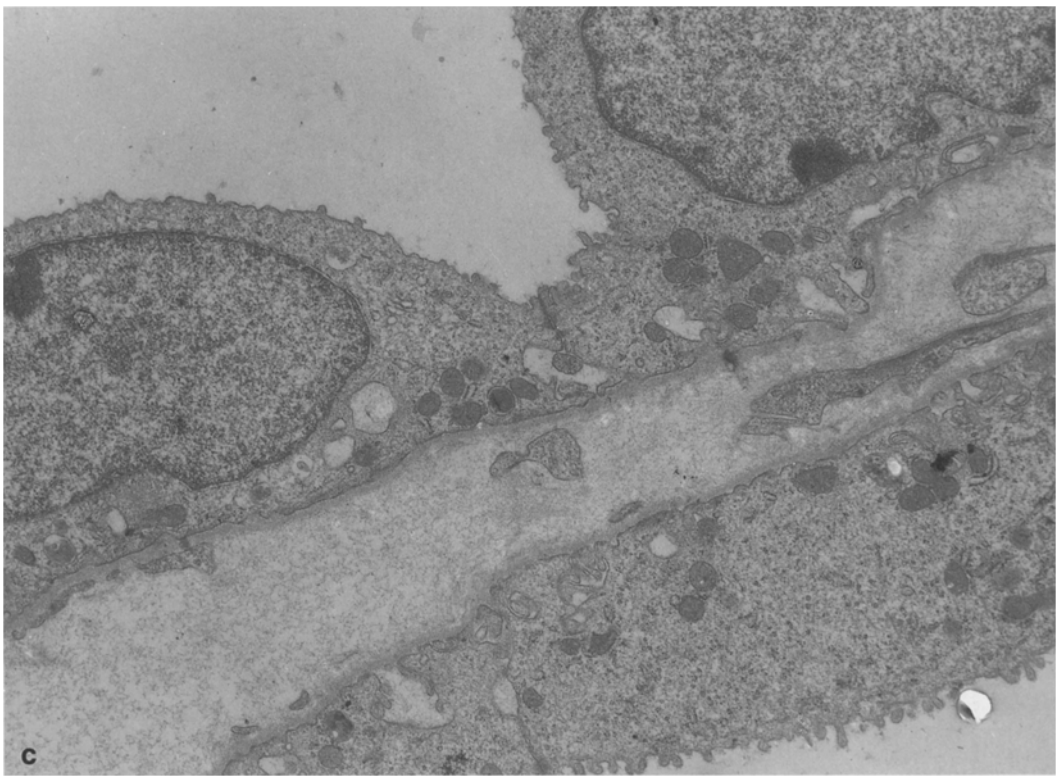

Fig. 2 C

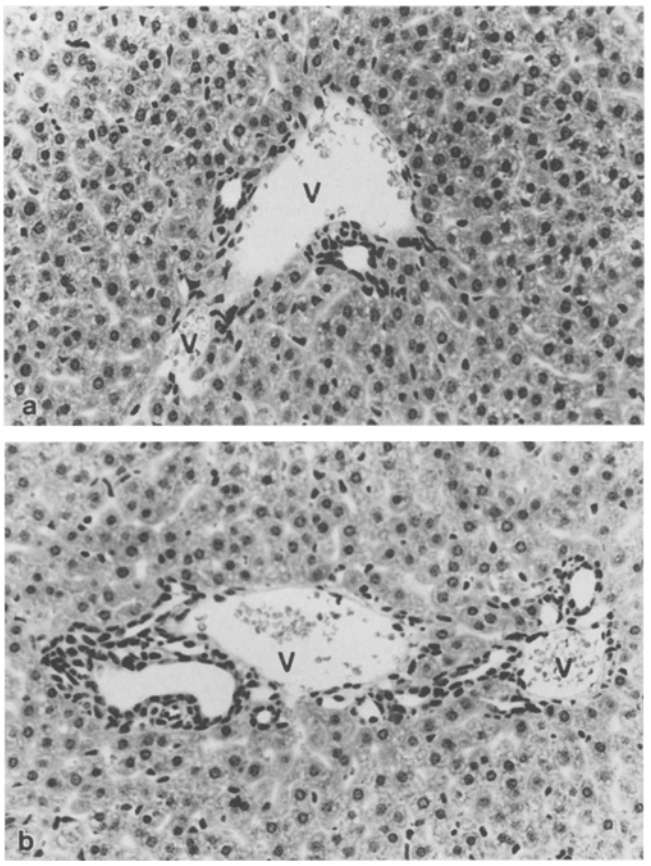

Fig. 3. Liver sections of 15-day-old mice (hematoxylin ×170). **A** A representative portal area in Balb/c control tissue with erythrocytes in the portal vein (*v*), accompanied by two bile ducts. **B** A representative "chaotic" portal area in BPK tissue. Two portal veins (v) are accompanied by multiple, irregularly shaped bile ducts

collecting tubular features. The opposing lateral surfaces of cyst-lining cells were decreased and the interdigitation simplified both laterally and basally with replacement by small membrane-bound spaces at the basal and basolateral surfaces. Intratubular polyps, piling of cells, wall thickening, intercellular space expansion or luminal projections were not observed. Despite gross disruption of overall renal architecture in the latter stages of disease progression, the basal laminae were intact, unsplit and of normal thickness.

There was a significantly increased number of mitoses in cyst-lining epithelial cells from both early proximal cysts on day 0 and 5 and early collecting tubular cysts on day 5 and 10 (Table 2). Undilated tubules in cystic kidneys demonstrated mitotic indices similar to age- and segment-matched control tubules. The numbers of cystic collecting tubules on day 0 and of undilated collecting tubules in cystic kidneys on day 20 were insufficient to allow appropriate statistical analysis.

Liver

The liver size of 10-day-old BPK mice was not different from controls as determined by the ratio of wet liver weight to body weight (BPK 2.9 ± 0.12% , controls 2.8 ± 0.04%). Liver weight was not affected by the animal's sex at this age. Light microscopy revealed an increased frequency of "chaotic" portal areas in BPK mice. These consisted of portal areas where the portal vein was surrounded by multiple, irregularly shaped bile ducts and epithelial cell proliferation (Fig. 3). In a blinded study on 1 section of each of 6 15-day-old BPK and 6 control animals, a trained pediatric pathologist (J.R.) identified 8.3 ± 2.6 such portal areas in BPK and 2.3 ± 1.2 in control mice (P <0.01). No other

Table 3. Portal structures in standardized liver sections at different postnatal developmental stages[a]

		DAY 5	DAY 15	DAY 25
Surface area (mm²)	Control	19 (6)	39 (2)	55 (9)
	BPK	28 (3)	40 (8)	51 (12)
Veins/mm²	Control	8.7 (1.8)	7.7 (1.2)	6.4 (0.9)
	BPK	6.8 (1.2)	8.0 (0.7)	7.0 (1.1)
Cells/mm²	Control	27 (8)	29 (8)	21 (5)
	BPK	40 (19)	45 (6)*	43 (10)**
Cells/Bile ducts	Control	16 (4)	14 (1)	11 (2)
	BPK	15 (5)	12 (1)	11 (2)
Bile ducts/mm²	Control	1.7 (0.3)	2.1 (0.5)	2.0 (0.3)
	BPK	2.6 (0.7)	3.7 (0.5)**	3.8 (1.0)**
Bile duct/Portal area	Control	1.5 (0.2)	1.4 (0.1)	1.3 (0.1)
	BPK	2.5 (0.5)**	1.6 (0.2)	1.7 (0.3)
Portal area/mm²	Control	1.1 (0.2)	1.4 (0.4)	1.5 (0.2)
	BPK	1.0 (0.1)	2.3 (0.2)**	2.3 (0.6)**
Portal area/100 veins	Control	13 (2)	18 (3)	23 (3)
	BPK	15 (2)	28 (2)**	32 (6)**

* P <0.05
** P <0.01 vs. controls
[a] Mean with SD in parentheses

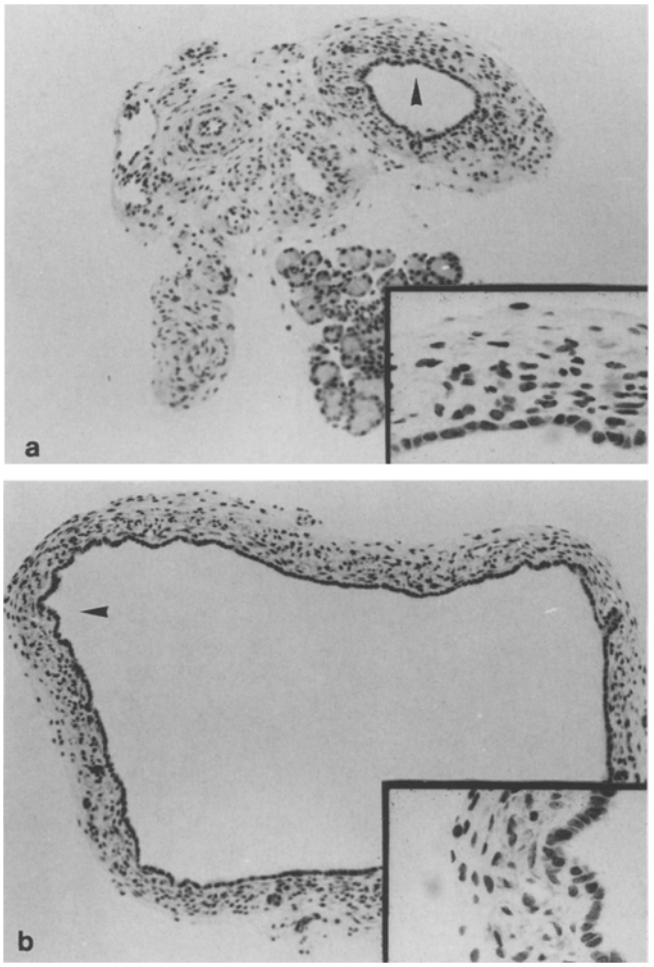

Fig. 4. Common bile ducts of 15-day-old mice (hematoxylin ×120). The area indicated by an *arrowhead* is shown at higher power (×250) in the insert. **A** Tissue from a control Balb/c mouse with some attached connective and pancreatic tissue. **B** The common bile duct of an affected BPK mouse. Note the normal cellular composition of the duct wall compared with control tissue (*insert*)

abnormalities were seen. There were no cystic abnormalities or signs indicative of portal or periportal fibrosis. Staining for bile was negative in all sections.

Ultrastructurally, the intrahepatic ducts in the BPK and age-matched control mice were lined by similar, morphologically normal epithelium. Cell organelles, junctions, appositions and basement membranes were unremarkable. The hepatocytes exhibited no evidence of bile inspissation or blunting of canalicular microvilli and had a normal distribution of hepatocellular organelles.

Counting of portal structures

Standardized liver sections from age-matched control and BPK animals, obtained for the counting of portal structures, were comparable with regard to section size and number of vein profiles (Table 3). During postnatal development considerable liver growth was accompanied in both strains by an increase in recognized portal areas (veins accompanied by bile ducts), a decrease of bile ducts per portal area and a decrease of epithelial cells per bile duct ($P < 0.05$ for all three age effects).

In BPK tissue there was marked epithelial hyperplasia. Biliary epithelial cells were increased by 50% on day 5, by 60% on day 15 and by 100% on day 25 when expressed per square millimeter of the section and compared with control values. This was associated with an increased number of bile ducts per square millimeter. Proliferation of bile ducts in BPK animals occurred in different patterns in the different postnatal age groups. In 5-day-old mice it was associated with an increase in bile ducts per portal area, while the number of portal areas was normal. In older animals bile duct proliferation was associated with an increased number of recognized portal areas.

Quantitation of bile duct shapes

Despite the earlier noted increase in "chaotic" portal areas in BPK mice, computerized morphometric analysis did not reveal any consistent abnormalities in bile duct surface area, circumference or "shape factor." Subgroups of bile duct profiles categorized according to their shape factor were represented equally in control and BPK livers. Casts of the intrahepatic biliary tree of 20-day-old BPK mice were not different from controls. No cysts, dilatations or von Meyenburg complexes were identified.

Extrahepatic biliary tract

Dilatation of the cystic, the hepatic and the common bile ducts was clearly visible after laparotomy in all postnatal homozygous BPK animals. This finding was linked to the presence of renal cysts in all instances. The outer diameter of the common bile duct was <0.25 mm in all control mice and between 0.4 and 1.5 mm in BPK mice ($P < 0.01$). No gender difference was noted. The duct walls of dilated bile ducts demonstrated cellular profiles which were not different morphologically from normal bile ducts, other than an increased number of epithelial cells (Fig. 4). Ultrastructurally the dilated ducts were lined by intact cuboidal epithelium with an intact microvillar surface. Apical tight junctions gave way to complex interdigitations of the lateral cell membranes. Cytoplasmic organelles were dispersed throughout the cell. The underlying basement membrane was unfrayed and of normal caliber and underlaid by collagen and fibroblasts with an active endoplasmic reticulum. The ultrastructural morphology did not differ from controls (Fig. 5). The gallbladder was not dilated and had a normal histology. The weights of the sutured undrained gallbladder in 10-day-old BPK and control mice were 0.9 ± 0.2 mg and 1.2 ± 0.6 mg, respectively.

Choledochoduodenal junction

Light microscopy of the choledochoduodenal junction did not reveal any abnormalities. The intraduodenal segment of the common bile duct was serially sectioned and found to be open and free of stenosis, fibrosis and inflammation.

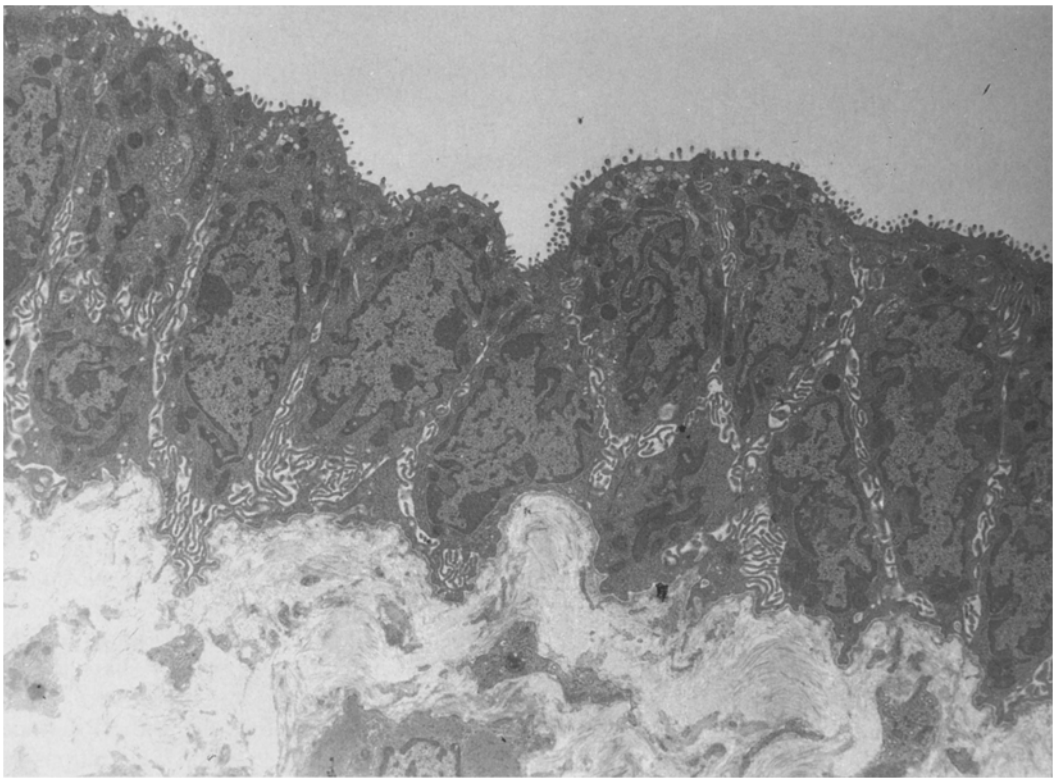

Fig. 5. Epithelial lining of a dilated common bile duct from a 30-day-old BPK mouse. The cell features are not distinguished from control ductal epithelium including superficial microvilli, apical organelles and extensive basolateral infoldings (× 5,300)

There was no restriction of the bile flow into the duodenum as measured by pressure-flow studies. The calculated resistances at 10 days of age were 4, 4, 6 and 8 cm/µl per second in BPK mice and 6, 7, 9 and 14 cm/µl per second in control mice.

Light microscopy of organs other than kidney or liver was unremarkable. No cystic or other abnormalities were seen and there were no signs of inflammation or fibrosis.

Discussion

The BPK mouse demonstrates autosomal recessive progressive tubular cyst formation associated with biliary abnormalities. This association is a well-recognized feature of the human ARPKD/CHF disease complex [9]. At one end of the clinical spectrum are patients with "classic" ARPKD who present neonatally with renal failure, only microscopic hepatic abnormalities and no clinical symptoms of liver disease. At the other end, are patients with CHF, presenting in early childhood with symptoms of portal hypertension and cholangitis but with normal renal function and only microscopic renal lesions. The clinicopathological classification of ARPKD introduced by Blyth and Ockenden [6] was based on the variable degree of renal and hepatic involvement as well as the age at presentation. It is now accepted that the different clinical entities introduced by Blyth and Ockenden [6] are different manifestations of the same genetic defect [5, 9]. The increased survival of even very young patients undergoing treatment for end-stage renal disease, in concert with the progressive nature of the hepatic abnormalities in ARPKD, leads to the expectation that many of these patients may eventually develop portal hypertension and progressive liver fibrosis. Therefore hepatic lesions are not only inherent to human ARPKD but also of increasing clinical importance.

Studies of the pathophysiology of human ARPKD are hampered by its low incidence, variable clinical expression and advanced pathology at presentation. As a consequence, research has largely focused on animal models. The animal model studied most extensively to date is the CPK mouse strain which expresses a lethal ARPKD much like the human disease [12, 17, 18, 28]. However, the validity of this model has been questioned since, unlike its human counterpart, biliary abnormalities could not be demonstrated in affected animals. Extensive studies identified hepatic cysts only in aged heterozygous breeders of the CPK strain, but not in homozygous animals with renal cysts [19, 20]. The invariably present biliary abnormalities demonstrated in cystic BPK mice not only emphasize the value of this strain as a new model of dual organ epithelial pathophysiology in ARPKD but also suggest it may have value as a model for the study of biliary dysgenesis.

The pattern of renal cyst formation and the progression of renal failure in the BPK strain are similar to those described for the CPK strain and, in latter stages, to those of human ARPKD. The two murine models demonstrate similar ultrastructural features of cyst-lining epithelium, although dilatation of intercellular spaces, previously noted in proximal tubular lesions of CPK animals [12], was not a feature of BPK mice. The localization of cysts to lectin-defined segments has yielded a number of interesting observations. The lesions in early stages of disease in BPK mice consist of dilatations exclusively localized to proximal tubules. These proximal tubular cysts most likely develop

in functioning, nonobstructed nephrons, as indicated by the normal cellular ultrastructure. This is consistent with microdissection data from the CPK model [12]. The contribution of proximal tubular cysts to the total population of cysts decreases during disease progression. This is most likely due to restriction of proximal tubular cystogenesis to a specific developmental stage in the context of ongoing nephrogenesis and progressive formation of collecting tubular cysts [12]. Regression of proximal tubular cysts has never directly been demonstrated in vivo, but has been demonstrated in vitro [29, 30]. Although proximal tubular cyst formation has not yet been demonstrated as an early feature of human ARPKD, it should be emphasized that little tissue from early disease stages has been available for detailed microdissection or lectin profiling analysis. Of particular interest in this respect is a recent histopathological study of ARPKD kidneys in which two of five specimens demonstrated slight positive staining for lectin markers specific for proximal tubules [31].

The histological picture of latter BPK disease stages is dominated by collecting tubular cysts. This is similar to data from patients with end-stage ARPKD in which systematic immunohistological and microdissection studies have localized most cysts to collecting tubular segments [12, 32]. In addition to proximal tubular cysts and collecting tubular cysts, there was a small population of BPK cysts which could not be localized by lectin profiling to either one of these segments (Table 1). Whether these cysts originate from a different nephron segment or represent phenotypic changes of preexisting proximal or collecting tubular cysts can only be determined by further studies. Involvement of nephron segments other than the proximal tubule or the collecting duct has not been suggested by ultrastructural analysis in the BPK strain and does not play a role in the cystogenesis of the CPK strain or ARPKD.

The intrahepatic abnormalities in standardized liver sections of BPK mice consist of hyperplasia of the biliary tract and an increased number of "chaotic" portal areas. In human CHF and related liver disorders, similar lesions have been described and attributed to a defective remodelling of the ductal plate [11]. According to current views, this plate is formed during normal liver development by transformation of hepatocytes into a double epithelial sheet surrounding the intrahepatic portal veins. During further development, this plate is then remodelled into multiple and later single bile ducts. The increased number of bile ducts and the abnormal shapes of bile duct profiles in liver sections of patients with ARPKD or CHF have been attributed to insufficient breakdown of the ductal plate and an arrest of the normal remodelling process [11]. The demonstrated increased number of bile ducts per portal area in early BPK disease stages is consistent with a remodelling defect, such that remodelling of the ductal plate has started but not been completed to the stage of single bile ducts. Further, the accelerated postnatal development of the biliary tract along the portal venous tract in BPK mice, indicated in our data by the increasing numbers of portal areas relative to controls, suggests additional abnormalities of the ductal plate remodelling process. Whether the multiple, irregular-shaped bile ducts observed in a limited number of portal areas from affected mice represent the curving biliary plates described for the "ductal plate malformation" in human disease by Jorgensen [13] cannot be concluded from this study. A separate study utilizing stereological reconstruction from serial sections is required to resolve this issue.

The observation in this study of an increased number of "chaotic" portal areas consisting of abnormal numbers and shapes of bile duct profiles was made by an experienced observer in a blinded study. It was therefore surprising and in contrast to data from human studies that no consistent abnormalities in bile duct shape or size could be demonstrated by quantitative morphometry [33]. It appears that the number of "chaotic" portal areas relative to the number of normal portal areas was insufficient to affect the quantitative morphometric analysis. The absence of intrahepatic fibrosis and cystic biliary dilatations in BPK mice contrasts with data from most patients with advanced CHF and related disorders [3, 9, 34]. It should be emphasized, however, that the early lethality of the renal disorder in the murine model necessarily restricted this study to early stages of liver disease.

Dilatations of the entire extrahepatic biliary tract, with the exception of the gallbladder, were strikingly present in all animals with cystic kidneys at all postnatal ages and never seen in unaffected animals. Biliary outflow restriction as the primary cause of this dilatation and of the intrahepatic biliary hyperplasia was excluded by the absence of gallbladder dilatation, normal serum bilirubin, the normal ultrastructure of the liver and common bile duct, and the normal resistance of the choledochoduodenal junction. Moreover, the massive luminal dilatation in conjunction with the apparently normally structured wall, in which increased numbers of biliary cells were paralleled by hyperplasia of the surrounding stroma, suggests a primary hyperplastic abnormality. Although the common bile duct dilatation invariably present in affected BPK animals has not been specifically associated with human ARPKD, it is a well-recognized finding in patients with Caroli's disease [35]. It thus appears that extrahepatic biliary dilatation is part of the variable hepatobiliary phenotypic expression of the ARPKD/CHF disease complex.

The renal and hepatic abnormalities demonstrated in this model suggest a common pathogenetic pathway. In both organs, epithelial hyperplasia is an early feature of the lesions, although the specific patterns of renal and biliary hyperplasia are somewhat different. The hyperplasia of tubular cystogenesis and the hyperplasia of the extrahepatic bile duct both are associated with luminal dilatation. In contrast, intrahepatic biliary epithelial hyperplasia in affected BPK mice is expressed as an increased number of bile ducts and thus elongation, rather than dilatation of the biliary tract.

Differences in the three-dimensional structural consequences of hyperplasia in kidney and liver may reflect the fact that these organs are in different developmental stages at the time that lesions develop. Since the renal cystic lesions develop in a segment-specific pattern in preexisting, structurally normal nephrons [12], elongation of hyperplastic segments is anatomically restricted by the attachment at both ends to fixed normal tubular segments. Uncontrolled growth of cells in such spacially restricted

tubular segments would then lead to expansion perpendicular to the long axis of the tubules, i.e., dilatation. Similarly, elongation of the extrahepatic bile duct is restricted by the attachment to liver and duodenum, and thus localized cellular proliferation would lead to dilatation. In contrast, the proliferative elongation of the intrahepatic biliary tract is part of the pattern of normal murine postnatal development, as illustrated by our data from control mice (Table 3). The intrahepatic biliary tract is not physically restricted by attachment to other organ structures until the normal developmental process is complete. It would be of interest to know whether biliary hyperplasia continuing beyond the end-point of biliary tract development would lead to increased numbers of bile ducts per portal area and luminal dilatations, and whether such abnormalities would be accompanied by fibrotic changes in the portal areas as seen in human disease. At present, such a course of events can only be speculated since affected BPK animals die of renal failure prior to this developmental stage.

We conclude that the presence of intra- and extrahepatic biliary hyperplasia in conjunction with progressive, hyperplastic renal tubular cyst formation make the BPK mouse strain an excellent model for the study of the ARPKD/CHF disease complex.

Acknowledgements. A preliminary report of these findings was presented at the 1991 Annual Meeting of the American Society of Nephrology, and has appeared in abstract form [36]. These studies were supported by the Sophia Foundation for Medical Research in Rotterdam, the Dutch Kidney Foundation and grants no. DK34891 and DK44875 from the National Institutes of Health. We gratefully acknowledge Dr. R. Vernier who initially provided us with breeder stock of the BPK mouse strain.

References

1. Lieberman E (1971) Infantile polycystic disease of the kidneys and liver: clinical, pathological and radiological correlations and comparison with congenital hepatic fibrosis. Medicine (Baltimore) 50: 277–318
2. Murray-Lyon IM, Shilkin KB, Laws JW, Illing RC, Williams R (1972) Non-obstructive dilatation of the intrahepatic biliary tract with cholangitis. Q J Med 164: 477–489
3. Alvarez F, Bernard O, Brunelle F, Hadchouel M, Leblanc A, Odièvre M, Alagille D (1981) Congenital hepatic fibrosis in children. J Pediatr 99: 370–375
4. Kaplan BS, Fay J, Shah V, Dillon MJ, Barratt TM (1989) Autosomal recessive polycystic kidney disease. Pediatr Nephrol 3: 43–49
5. McDonald R, Avner ED (1991) Cystic disease in children. Semin Nephrol 11: 632–642
6. Blyth H, Ockenden BG (1971) Polycystic disease of kidneys and liver presenting in childhood. J Med Genet 8: 257–284
7. Resnick J, Vernier RL (1987) Renal cystic disease and renal dysplasia. In: Holliday MA, Barratt TM, Vernier RL (eds) Pediatric nephrology, 2nd edn. Williams and Wilkins, London, pp 371–383
8. Summerfield JA, Nagafuchi Y, Sherlock S, Cadafalch J, Scheuer PJ (1986) Hepatobiliary fibropolycystic diseases, a clinical and histological review of 51 patients. J Hepatol 2: 141–156
9. Picolli DA, Witzleben CL (1991) Disorders of intrahepatic bile ducts. In: Walker WA, Durie PR, Hamilton JR, Walker-Smith, Watkins JB (eds) Pediatric gastrointestinal disease, vol 2. Decker, Philadelphia, pp 1124–1140
10. Kaplan BS, Kaplan P (1990) Autosomal recessive polycystic kidney disease. In: Spitzer A, Avner ED (eds) Inheritance of kidney and urinary tract diseases. Kluwer, Dordrecht, pp 265–276
11. Desmet VJ (1985) Intrahepatic bileducts under the lens. J Hepatol 1: 545–549
12. Avner ED, Studnicki FE, Young MC, Sweeney WE Jr, Piesco NP, Ellis D, Fetterman GH (1987) Congenital murine polycystic disease. I. The ontogeny of tubular cyst formation. Pediatr Nephrol 1: 587–596
13. Jørgensen MJ (1977) The ductal plate malformation. Acta Pathol Microbiol Scand A [Suppl] 257: 1–88
14. Avner ED, Sweeney WE, Nelson WJ (1992) Abnormal sodium pump distribution during renal tubulogenesis in congenital murine polycystic kidney disease. Proc Natl Acad Sci USA 89: 7447–7451
15. Harding MA, Chadwick LJ, Gattone VH, Calvet JP (1991) The SGP-2 gene is developmentally regulated in the mouse kidney and abnormally expressed in collecting duct cysts in polycystic kidney disease. Dev Biol 146: 483–490
16. Avner ED, McAteer JA, Evan AP (1990) Models of cysts and cystic kidneys. In: Gardner KD, Bernstein J (eds) The cystic kidney. Kluwer, Dordrecht, pp 55–98
17. Avner ED, Sweeney WE Jr, Young MC, Ellis D (1988) Congenital murine polycystic kidney disease. Pediatr Nephrol 2: 210–218
18. Fry JL, Koch WE, Jennette JC, Mc Farland MA, Mandel J (1985) A genetically determined murine model of infantile polycystic kidney disease. J Urol 134: 828–833
19. Crocker JFS, Blecher SR, Givner ML, McCarthy SC (1987) Polycystic kidney and liver disease and corticosterone changes in the cpk mouse. Kidney Int 31: 1088–1091
20. Grimm PC, Crocker JFS, Malatjalian DA, Ogborn MR (1990) The microanatomy of the intrahepatic bile duct in polycystic disease: comparison of the cpk mouse and human. J Exp Pathol 71: 119–120
21. Laitinen L, Virtanen I, Saxén L (1987) Changes in the glycosylation pattern during embryonic development of mouse kidney as revealed with lectin conjugates. J Histochem Cytochem 35: 55–65
22. Avner ED, Sweeney WE Jr (1990) Polypeptide growth factors in metanephric growth and segmental nephron differentiation. Pediatr Nephrol 4: 372–377
23. Van Eyken P, Sciot R, Desmet VJ (1988) Intrahepatic bile duct development in the rat: a cytokeratin-immunohistochemical study. Lab Invest 59: 52–59
24. Sweeney WE Jr, Avner ED (1991) Intact organ culture of murine metanephros. J Tissue Cult Methods 13: 163–168
25. Morris SM, Sweeney WE, Kepka DM, O'Brien WE, Avner ED (1991) Localization of arginine biosynthetic enzymes in renal proximal tubules and abundance of mRNA during development. Pediatr Res 28: 1151–1154
26. Acker CJ, Mitchel D (1987) Sigmascan manual. Jandel Scientific, Sausolito, California, pp 3.28–3.34
27. Woodbury PW, Mitchell ME, Scheidler DM, Adams MC, Rink RC, McNulty A (1989) Constant pressure perfusion: a method to determine obstruction in the upper urinary tract. J Urol 142: 632–635
28. Preminger GM, Koch WE, Fried FA, Mc Farland E, Murphy ED, Mandell J (1982) Murine congenital polycystic kidney disease: a model for studying development of cystic disease. J Urol 127: 556–560
29. Avner ED, Sweeney WE Jr, Piesco NP, Ellis D (1986) Regression of genetically determined polycystic kidney disease in murine organ culture. Experientia 42: 77–80
30. Avner ED, Sweeney WE Jr, Ellis D (1989) In vitro modulation of tubular cyst regression in murine polycystic kidney disease. Kidney Int 36: 960–968
31. Verani R, Walker P, Silva FG (1989) Renal cystic disease of infancy: results of histochemical studies. Pediatr Nephrol 3: 37–42
32. Holthofer H, Kumpulainen T, Rapola J (1990) Polycystic disease of the kidney. Evaluation and classification based on nephron segment and cell-type specific markers. Lab Invest 62: 363–369
33. Jørgensen MJ (1973) A stereological study of intrahepatic bile ducts. Acta Pathol Microbiol Scand A 81: 670–675
34. Kerr DNS, Harrison CV, Sherlock S, Milnes Walker R (1961) Congenital hepatic fibrosis. Q J Med 30: 91–117
35. Caroli J, Corcos V (1964) Maladies des voies biliaires intrahépatiques segmentaires. Masjon and Cie, Paris
36. Nauta J, Sweeney WE, Avner ED (1991) Epithelial hyperplasia and cell polarity abnormalities in murine autosomal recessive polycystic kidney disease (abstract). J Am Soc Nephrol 2: 257